Horizontal Sound Field Reproduction with Point Sources using Distributed Constraints

D. Menzies

De Montfort University, Email: rdmg@dmu.ac.uk

Abstract

A preliminary investigation is presented of horizontal sound field control using a rectangular array of spherical wave driving sources, with focus on wide area plane wave reproduction. Comparison is made between Wave Field Synthesis and a method based on distributed pressure and velocity constraints. Advantages of the second approach are discussed, and modifications of the both methods are proposed.

Introduction

Horizontal sound field reproduction with point driving sources using either Wave Field Synthesis (WFS) [1, 2, 3] or High Order Ambisonics (HOA) [4, 5] suffers from reproduction errors that do not fall to zero as the number of drivers is increased. The error is unsurprising because a 3D source restricted to the plane is not a solution of the 2D wave equation, most obviously because the 2D field divergence is not zero around the 3D source. A line array with 3D drivers can be analyzed fully because of its symmetry, however it is not immediately clear what is possible with more general arrays. In an attempt to find better solutions a distributed constraint (DC) method is investigated here following on from related work using 2D and 3D drivers for 2D and 3D control. Simulations are used to compare the fields generated using WFS and DC. The test fields used are plane waves, which are harder to reproduce accurately than virtual point source fields due to the use of more drivers. The arrays used are rectangular which is a common practical configuration, particularly in concert halls. From the scattering view in the Simple Source formulation [6], driving functions are expected to be more complex for boundaries with sharper corners.

Reproduction methods

Distributed constraints

Previously the control of 2D sound fields was considered by applying modal constraints on a grid of points in the target region [7]. This is effective because the constraints at each point can accurately describe a sound field region of any radius. In 3D with a horizontal array the contribution from each driver at a point in the array plane cannot be expressed in a 2D modal expansion. Of course it is possible to apply derivative constraints of any order, but the non-attainability of the solution implies that higher-order constraints will dominate the error and the problem will be over-constrained. For this reason only pressure and gradient constraints are given at each point in the target region. This is equivalent to constraint by the horizontal components of the first order Fourier-Bessel expansion.

The set of all constraints can be written at each frequency as

$$c_{ln} = \sum S_{jn}(\boldsymbol{r}_{s_j} - \boldsymbol{r}_{c_l}) s_j = \sum M_{lnj} s_j \quad . \tag{1}$$

where c_{ln} are the pressure and horizontal gradient, indexed by n at each constraint point, indexed by l. s_j are the driving functions to be determined. $S_{jn}(\boldsymbol{r}_{s_j} - \boldsymbol{r}_c)$ are the pressure and horizontal gradient of the jth driver field located at $\boldsymbol{r}_{s_j} - \boldsymbol{r}_c$ relative to the measurement point. $\boldsymbol{r}_{s_j}$ and $\boldsymbol{r}_c$ are the locations of the sources and the constraints respectively. In the case of monopole drivers assumed in this study, the driver field descriptions are identical, $S_{jn} = S_n$.

The driving functions are found by finding the pseudo inverse of M_{lnj} with l and n grouped into one index,

$$s = \bar{M}^{+} \bar{c} \quad . \tag{2}$$

Basic Tikhonov regularization is used, so that M^+ is the regularized pseudo inverse $(M^T M + \alpha^2 I)^{-1} M^T$, with parameter α.

The driver normalization used is $e^{ikr}/4\pi r$, the same as that matching (4). This allows the driving function levels to be compared directly. The gradient of the driving field in the horizontal plane is equal to the total gradient,

$$\nabla \frac{e^{-ikr}}{4\pi r} = -(ik + \frac{1}{r}) \frac{e^{-ikr}}{4\pi r} \hat{\boldsymbol{r}} \quad . \tag{3}$$

This is equivalent to the horizontal components in the first order Fourier-Bessel expansion of the field. having the same r dependence given by the spherical hankel function, $h_1^{(2)}(kr)$.

Wave Field Synthesis

WFS is a well established method for efficiently calculating and applying driving functions for the synthesis of virtual sources. For the synthesis of a plane wave $e^{-i\boldsymbol{k}\cdot\boldsymbol{r}}$ on a horizontal array the continuous driving function is [3]

$$D_{pw,2.5}(\boldsymbol{x}_0,\omega) = -2a_{pw}(\boldsymbol{x}_0)\sqrt{2\pi|\boldsymbol{x}_{ref}-\boldsymbol{x}_0|}\times$$
$$\times\sqrt{i\frac{w}{c}}\hat{S}_{pw}(\omega)\boldsymbol{n}_{pw}^T\boldsymbol{n}(\boldsymbol{x}_0)e^{-i\frac{\omega}{c}\boldsymbol{n}_{pw}^T\boldsymbol{x}_0} \quad (4)$$

This is sampled at each driver point with an extra factor δ_s, the driver spacing, included to match the level of the continuous driver reproduction. The driving function consists of a driver independent filter, and driver dependent gain and delay terms.

Simulations

For convenience length units are chosen so that the highest frequency considered, the WFS alias / Nyquist frequency, has wavelength $\lambda = 1$. The array spacing is then $\lambda = 0.5$. The test array used has dimensions 10×10. The length in metres of the array spacing used in WFS systems is typically $0.10m$ to $0.3m$ corresponding to a Nyquist frequency of $\approx 1000Hz$. The real arrays with this spacing corresponding to the test arrays would have dimensions $\approx 4m \times 4m$. Although concert halls can be several times larger than this, the results will provide a useful guide.

The first set of simulations show the reproduction of a plane wave traveling at two angles, $0°, 45°$ relative to the right pointing direction. These are repeated for WFS and DC, and for $\lambda = 1, 4$, Figures 1,2,3,4,5,6,7,8. For DC the constraints are placed on a square grid with spacing 0.25 . The grid is separated from the boundary by a margin of distance 1. For each simulation the following plots are shown : the real value of the reproduced complex pressure field $P(\boldsymbol{x},\omega)$; the relative error $\epsilon(\boldsymbol{x},\omega) = |P(\boldsymbol{x},\omega)-P_t(\boldsymbol{x},\omega)|/P_t(\boldsymbol{x},\omega)$ where $P_t(\boldsymbol{x},\omega)$ is the target; and the absolute value $|P(\boldsymbol{x},\omega)|$ expressed in dB. The target planewave is 0 dB everywhere. Also shown on the top line of each figure is $\max(s)$, the maximum absolute value of the driving function, as an indication of driver energy level.

The DC simulations show good coverage and wavefront stability, and level fade in the direction of travel that is significantly reduced relative to WFS. Directional imaging stability is indicated by the variation of the wave gradient direction, which is clearly visible. The WFS simulations exhibit the level fade known from line arrays, and also a narrowing of width. The small scale instability can be nearly removed at $\lambda = 1$ by modifying the selection window so that it fades over distance 2 at each edge. At lower frequencies this approach is not completely effective, and instability remains, as would be expected from the Simple Source scattering picture. The narrowing effect worsens progressively as edge fade is introduced.

The next set of simulations shown in Figures 9,10,11,12 model a reduced target area, starting distance 4 from the left, which could represent a concert room with a stage area on the left where a coherent field is not required.

The increased freedom permits solutions with further

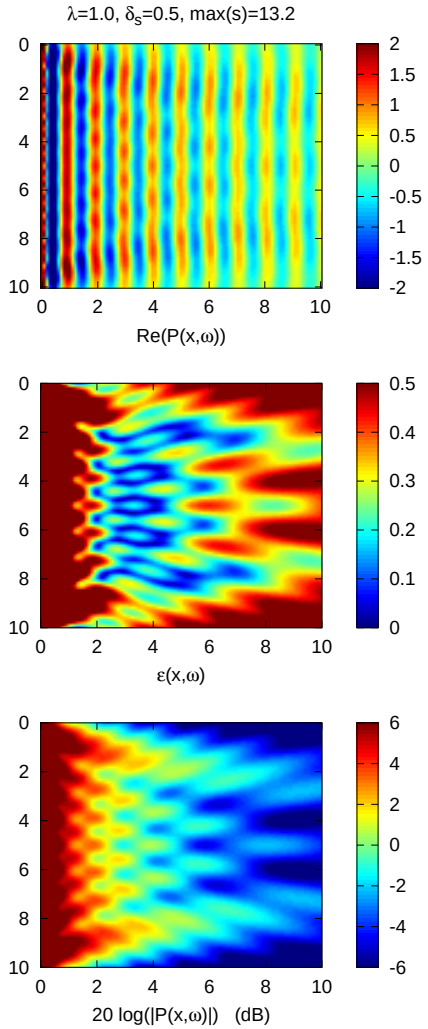

Figure 1: WFS reproduction, plane wave angle $0°, \lambda = 1$,

reduced fade and stable wavefronts, perhaps more than might be expected. Evidently the increased frontal distance working in combination with side sources is effective. Solutions for greater angles show more similar results to those found in the previous set, as would be expected.

WFS modification

It appears the availability of side drivers in DC is effective at compensating the narrowing effect seen in WFS, particularly at small angles. This suggests WFS might be modified by extending the driving function so it is active along the sides in order to reduce narrowing. A first attempt is given by the following modification of the dot product factor,

$$\boldsymbol{n}_{pw}^T\boldsymbol{n}(\boldsymbol{x}_0) \rightarrow (\boldsymbol{n}_{pw}^T\boldsymbol{n}(\boldsymbol{x}_0)+\gamma)/(1+\gamma) \quad . \quad (5)$$

The driving function is unchanged where the boundary faces in the direction of the plane wave. Simulations using this factor are shown in Figures 13,14

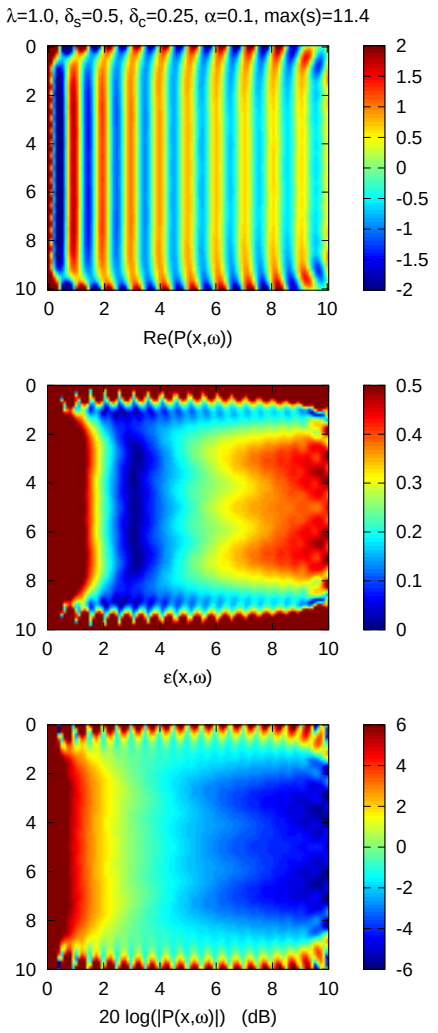

Figure 2: DC reproduction, plane wave angle $0°\lambda = 1$,

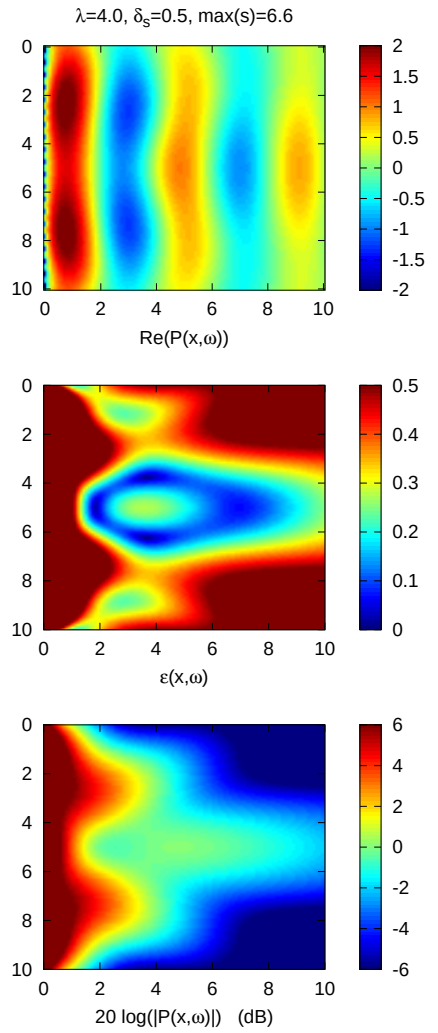

Figure 3: WFS reproduction, plane wave angle $0°\lambda = 4$,

Narrowing and fade is reduced at both frequencies shown. Wavefront stability is not very good but improves at the lower frequency. It appears that an approximate evanescent field produced by the sides is partly compensating for narrowing effect. This positive result raises the question of treating the main components of the WFS driving function, pre-delay, gain and delay as free parameters in order to optimize reproduction efficiently. The optimal control of the parameters might be encoded using efficient non-linear learning schemes, such as gaussian mixtures or neural networks. The control of Further more the driving function might be given more degrees of freedom, while remaining computationally efficient, for example by introducing an additional pre-filter:

$$D_l = (f_1(\omega)g_{1,l} + f_2(\omega)g_{2,l})e^{-iwt_l} \qquad (6)$$

Conclusion

The simulations have shown that at least for plane wave reproduction in rectangular boundaries DC can improve on the reproduction quality of WFS, in terms of stability, width narrowing and distance fade, over 3 octaves from the WFS alias frequency (not all shown). This suggests good broadband performance, however more simulations are needed to test pulse performance. Reduction of target area, for instance due to a stage area can give significant improvements over a range of angles.

The cost of both filter calculation and filter application is much higher in DC than in WFS, requiring FIR filtering. However it could be useful to pre-calculate filters for static sources. Furthermore, the playback of complete pre-rendered driving signal sets is possible from consumer computer equipment together with audio interfaces already in use with WFS systems. For sufficient rendering complexity it may eventually make sense to pre-render filter sets for basis fields covering the whole target area. Different methods can be combined, so for example combining near WFS sources with pre-rendered

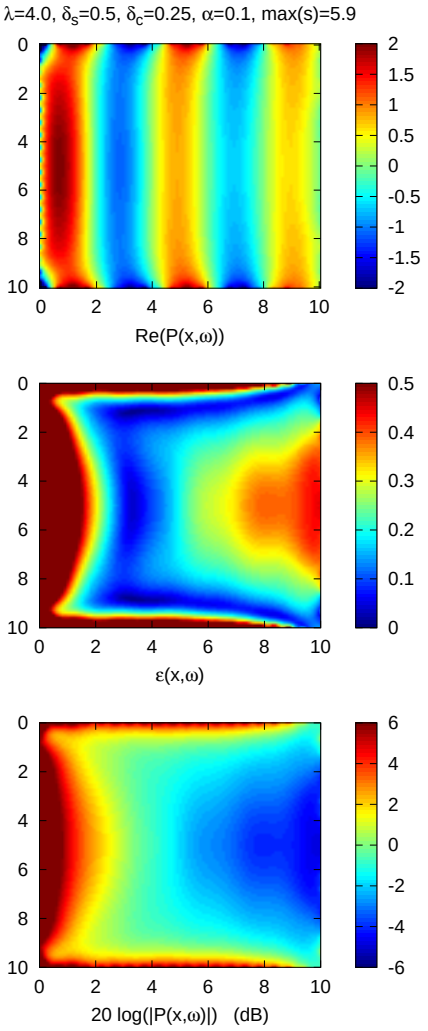

Figure 4: DC reproduction, plane wave angle $0°\lambda = 4$,

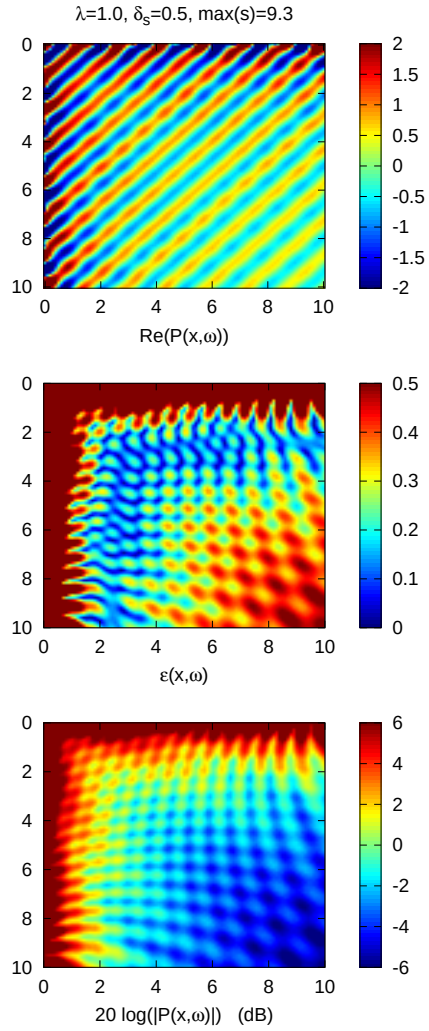

Figure 5: WFS reproduction, plane wave angle $45°, \lambda = 1$,

distant backgrounds.

Other areas for consideration are the modelling of speaker directivity to improve reproduction accuracy. Pre-fading the target solutions to more closely match what is possible may help to produce better solutions. Also it was shown that WFS itself can be modified without significant extra cost to give improved reproduction. There are many ways in which this could be further explored.

References

[1] A. J. Berkhout and P. de Vries, D.and Vogel, "Acoustic control by wave field synthesis," *J. Acoust. Soc. Am.*, vol. 93, pp. 2764–2778, 1993.

[2] E. Verheijen, "Sound reproduction by wave field synthesis," Ph.D. dissertation, Delft University of Technology, January 1998.

[3] S. Spors, R. Rabenstein, and J. Ahrens, "The theory of wave field synthesis revisited," in *Preprint 7358, AES 124th Convention, Amsterdam*, May 2008.

[4] M. A. Gerzon, "Periphony (with-height sound reproduction)," in *Proc. AES 2nd Convention, Munich*, 1972.

[5] J. Daniel, "Spatial sound encoding including near field effect," in *Proc. AES 23nd International Conference, Helsinger, Denmark*, 2003.

[6] E. Williams, *Fourier Acoustics: sound radiation and nearfield acoustical holography.* Elsevier, 1999.

[7] D. Menzies, "Sound synthesis for general enclosures," in *Proc. 2nd Int. Symposium on Ambisonics and Spherical Acoustics, IRCAM Paris*, May 2010.

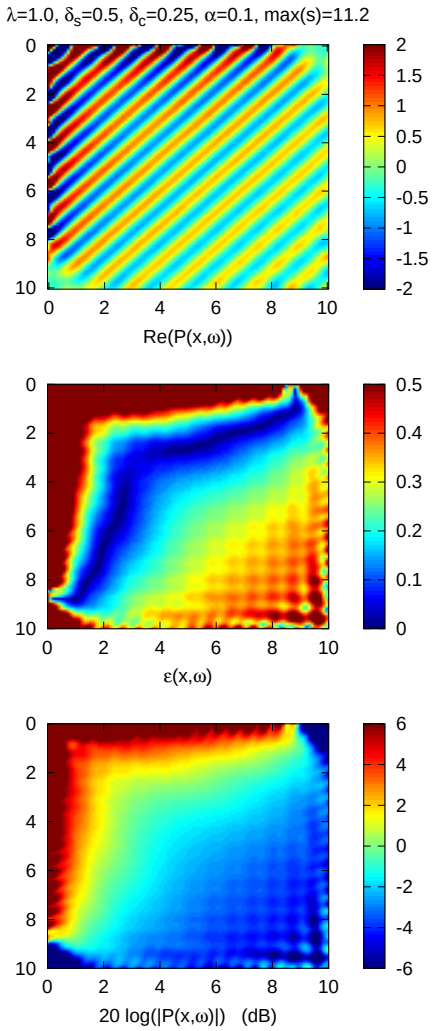

Figure 6: DC reproduction, plane wave angle $45^\circ\lambda = 1$,

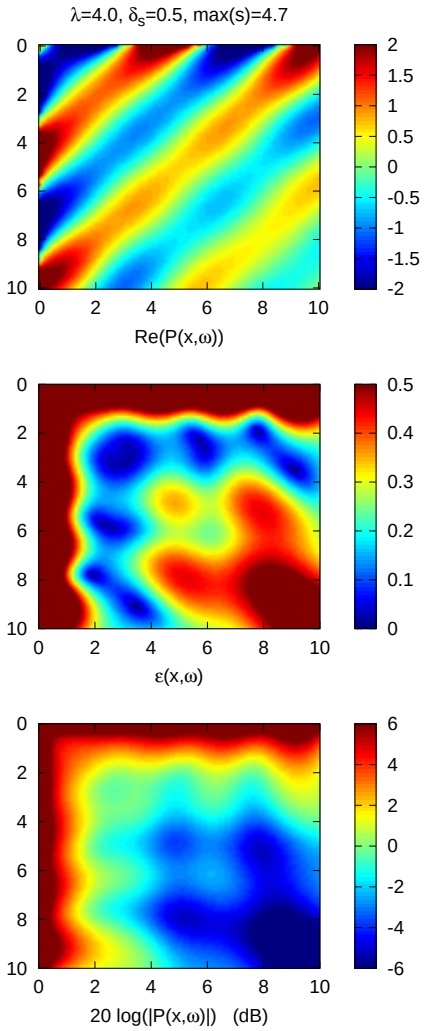

Figure 7: WFS reproduction, plane wave angle $45^\circ\lambda = 4$,

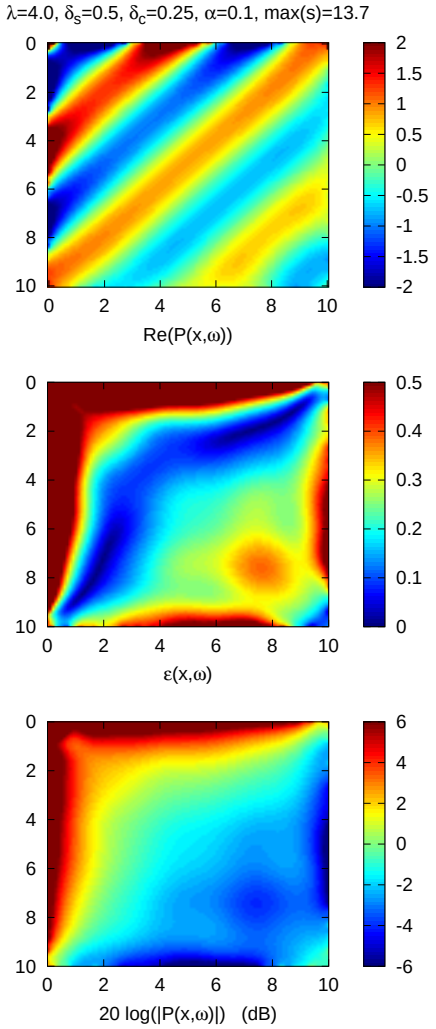

Figure 8: DC reproduction, plane wave angle $45^\circ \lambda = 4$,

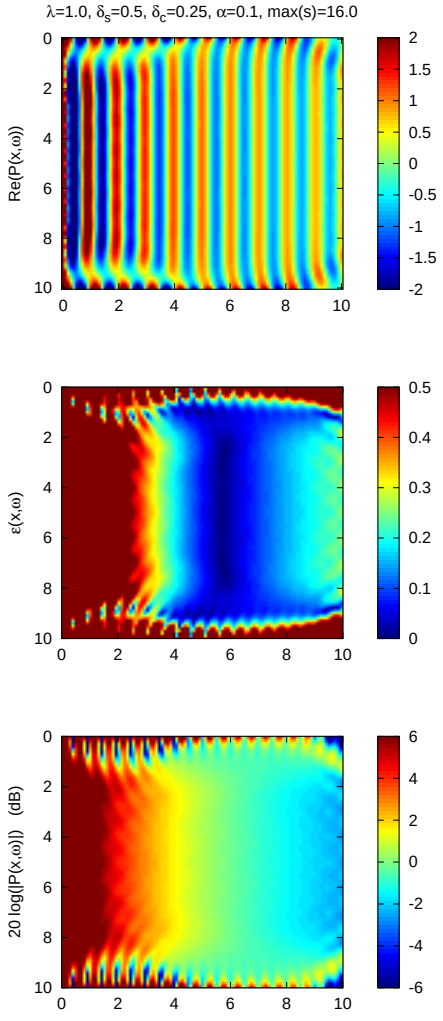

Figure 9: DC reproduction, reduced target, plane wave angle $0^\circ \lambda = 1$,

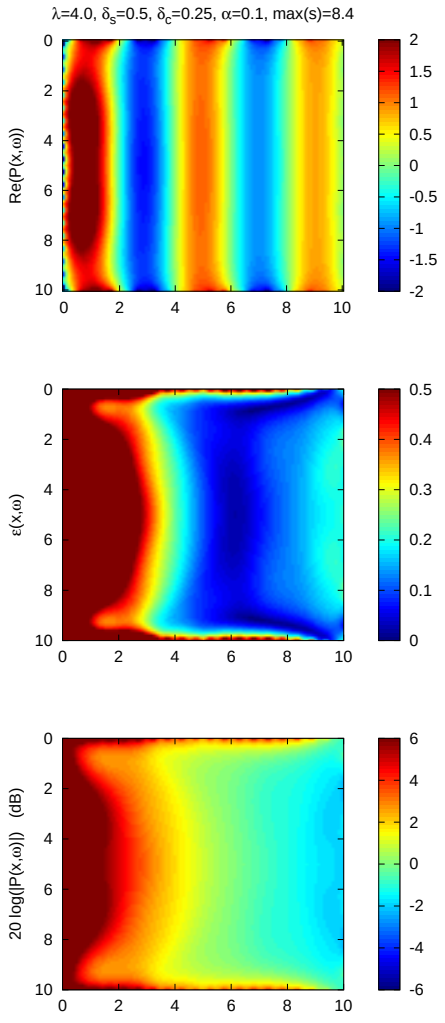

Figure 10: DC reproduction, reduced target, plane wave angle $0°\lambda = 4$,

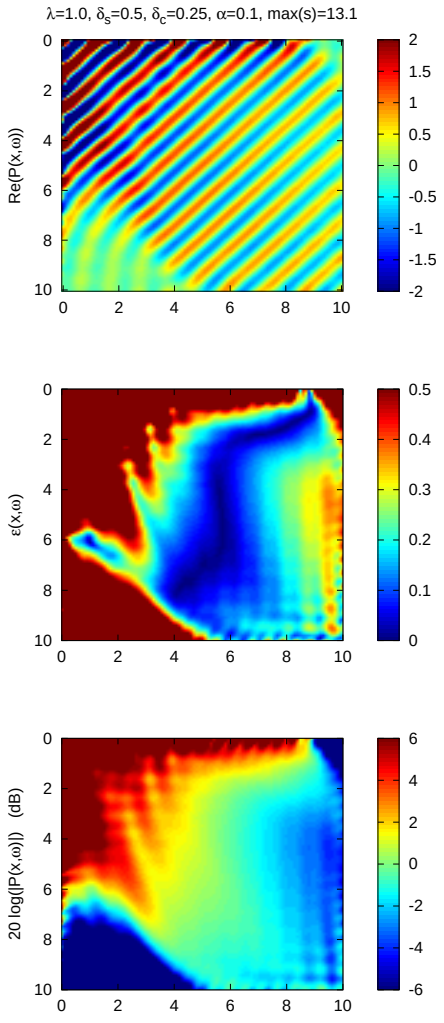

Figure 11: DC reproduction, reduced target, plane wave angle $45°\lambda = 1$,

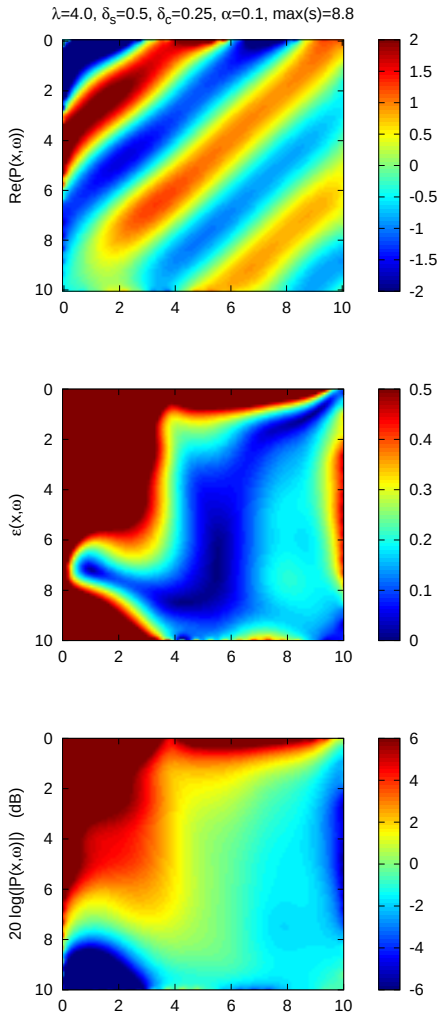

Figure 12: DC reproduction, reduced target, plane wave angle $45°\lambda = 4$,

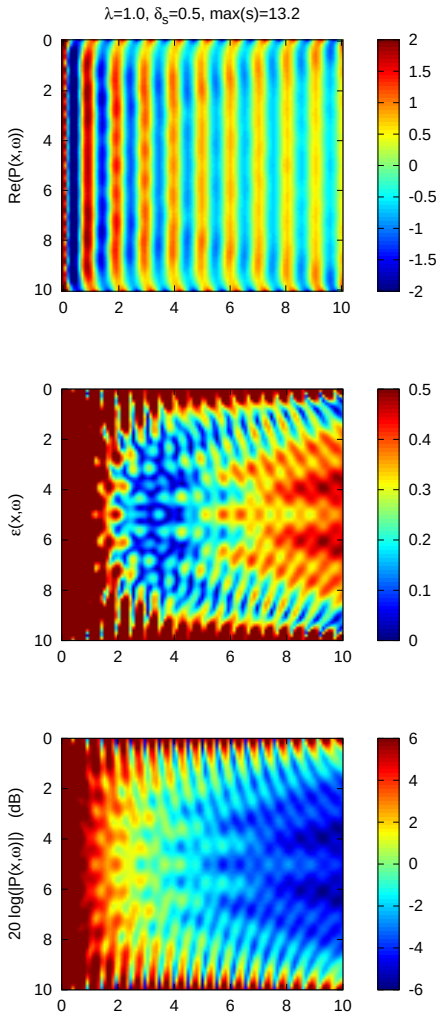

Figure 13: Modified WFS reproduction, $\gamma = 0.2$, plane wave angle $0°\lambda = 1$,

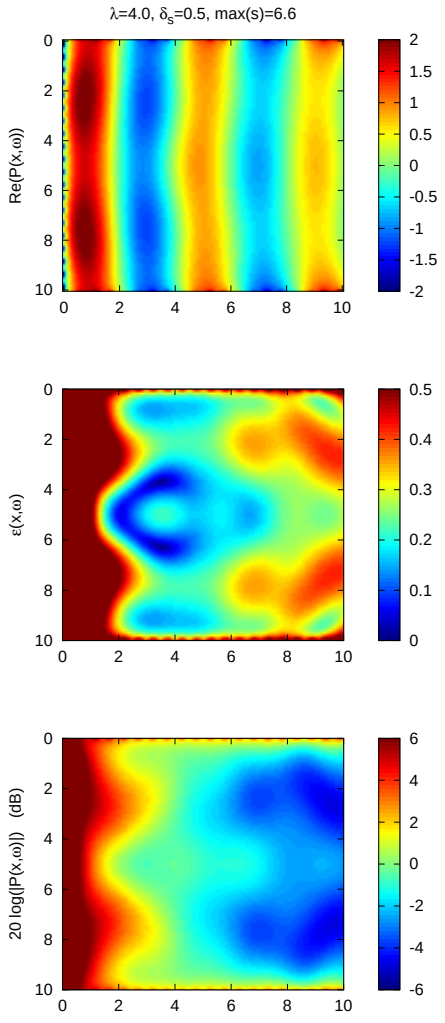

Figure 14: Modified WFS reproduction, $\gamma = 0.2$, plane wave angle $0° \lambda = 4$,